T.C.

ALTINBAŞ UNIVERSITY

Institute of Graduate Studies

Electrical and Computer Engineering

VISIBILE LIGHT COMMUNICATION CHANNEL ESTIMATION BASED ON NEURAL NETWORK

Raad Hammood Hasan ALDOORI

Master of Science

Supervisor

Asst. Prof. Ahad ARDABILI

Istanbul, 2021

VISIBILE LIGHT COMMUNICATION CHANNEL ESTIMATION BASED ON NEURAL NETWORK

by

Raad Hammood Hasan Aldoori

Electrical and Computer Engineering

Submitted to the Graduate School of Science and Engineering

in partial fulfillment of the requirements for the degree of

Master of Science

ALTINBAŞ UNIVERSITY

2021

The thesis titled “VISIBILE LIGHT COMMUNICATION CHANNEL ESTIMATION BASED ON NEURAL NETWORK” prepared and presented by “Raad Hammood Hasan ALDOORI” was accepted as a Master of Science Thesis in Electrical and Computer Engineering.

Asst. Prof. Ahad Khaleghi ARDABILI

Supervisor

Thesis Defense Jury Members:

Asst. Prof. Ahad Khaleghi ARDABILI	School of Engineering and Natural Sciences, Altinbas University	_____
Prof. Osman Nuri UÇAN	School of Engineering and Natural Sciences, Altinbas University	_____
Asst. Prof. Taymaz Rahkar FARSHI	Faculty of Software Engineering, Ayvansaray University	_____

I certify that this thesis satisfies all the requirements as a thesis for the degree of Master of Science.

Approval Date of Institute of Graduate Studies:
____/____/____

I hereby declare that all information in this document has been obtained and presented in accordance with academic rules and ethical conduct. I also declare that, as required by these rules and conduct, I have fully cited and referenced all material and results that are not original to this work.

Raad Hammood Hasan ALDOORI

Signature

DEDICATION

To the most precious thing I have in this world, "my father and my mother", who spent their youth in order to reach what I have reached,

To my dear wife who stood by me in all circumstances, To everyone who helped me and wished me good.

ACKNOWLEDGEMENTS

I thank and express appreciation to Dr. Ahad ARDABILI, my wonderful supervisor, for his encouragement and understanding during my work on my study. He did not spare any detail and he answered all my questions quickly. Thank you, I learned a lot with your efforts and hope I can fulfill your goals.

ABSTRACT

VISIBILE LIGHT COMMUNICATION CHANNEL ESTIMATION BASED ON NEURAL NETWORK

Aldoori, Raad Hammood Hasan

M.Sc., Electrical and Computer Engineering, Altınbaş University,

Supervisor: Ahad ARDABILI

Date: 1/2021

Pages: (48)

Visible light communication techniques are increasingly emerging to address these needs with growing criteria for easy and secure communication between devices. One of the main strategies using many links for high-performance, stable communication is multiple input and output (MIMO) systems. But the increased number of communication links adds to the difficulty of the channel calculation, which is necessary if transmitted data is to be correctly decoded. Therefore, it is important to improve detailed and effective methods of channel estimation. We disclose the performance of neural network channel estimation approaches to boost the performance of MIMO visible light channel estimation. The proposed estimation method compared with linear regression to check the accuracy of the proposed method. Simulation results of both NN and linear regression method compared and it's clear that the BER was in range of 10^{-5} for the NN which is better than the BER for linear regression method which was in range of 10^{-2}. The main advantage of using NN for VLC channel estimation is the reduction of SNR while keeping low BER. The estimation results show that the presented algorithm is comparable to the MATLAB standard channel model. The results confirm that this procedure can be used efficiently in channel estimation.

Keywords: Channel Estimation, Neural Networks, MIMO, Visible Light Communications, SNR, BER.

TABLE OF CONTENTS

LIST OF TABLES

Pages

LIST OF FIGURES

Pages

LIST OF ABBREVIATIONS

OWC	:	Optical wireless communications
FSO	:	Free space optical
VLCC	:	Visible light communication consort ion
VLC	:	Visible light communication
RF	:	Radio frequency
LED	:	Light emitting diode
MIMO	:	Multiple input multiple output
VL	:	Visible light
DD	:	Direct detection
Tx	:	Transmitter
Rx	:	Receiver
DSP	:	Digital signal processing
DAC	:	Digital to analog conversion
LD	:	Laser diode
APD	:	Avalanche photo diode
OTx	:	Optical transmitter
ORx	:	Optical receiver
CIR	:	Chanel impulse response
DC	:	Direct current
RMS	:	Root mean square
OOK	:	On off keying
OFDM	:	Orthogonal frequency division multiplexing
PAM	:	Pulse amplitude modulation
AWGN	:	Additive white Gaussian noise
RZ	:	Return to zero
NRZ	:	Non return to zero
PPM	:	Pulse position modulation
OPPM	:	Overlap pulse position modulation

MPPM	:	Multiple pulse position modulation
SC	:	Sub carrier
IFFT	:	Inverse fast Fourier transform
PDP	:	Power distribution profile
D2DC	:	Device to device communication
EM	:	Electromagnetic
PD	:	Photo diode
PC	:	Personal computer
SNR	:	Signal to noise ratio
LOS	:	Line of site
NN		Neural Network
PoE	:	Power over Ethernet

LIST OF SYMBOLS

Hz	:	Hertiz
nm	:	Nano meter
∞	:	infinity
h	:	Chanel DC gain
P_r	:	Received power
P_{ave}	:	Average power
D	:	dimension
S	:	Transmitted power
Wij	:	Weight of neuron

1. INTRODUCTION

1.1 BACKGROUND

Since ancient times, optical wireless communications (OWC) have developed as a promising technology for data communication in the form of optical telegraphs via torches, smoke signals, beacon fires and semaphore lines [7]. There are many possible uses of OWC and there is huge increase in uses. The OWC, also known as free space optical (FSO) systems, has succeeded in its use in recent decades for point-to-point external communication. Areas in which FSO has been used include high bit inter-construction connections over distances up to several kilometers[1]. The commercialization of OWC has had a substantial boost with respect to indoor applications in the 90s, with the establishment in 1993 of the Infrared Data Association (IrDA). IrDA has become a highly effective solution for file transfer between mobile devices and computers as well as remote television and video player controls[2]. The Visible light communication consortium (VLCC) was formed in 2003, with the objective of proposing standards for VLC and promoting the technology[3].

Recently, scholars and engineers have been very involved in optical Wireless Communications (OWC). Researchers have developed new technology in the fields of cables, such example as millimeters waves, free optical space and underwater audio communications, in tandem with the high demand of high data speeds of cell phones. One of the promising technologies considered for 5 G or higher networking requirements is visible light networking (VLC). VLC has many benefits in contrast with RF systems over 10,000 times wider and less limited bandwidth, reduced implementation costs, better coverage and less interference from other RF devices VLC has many advantages[4]. In the beginning of the 2000s, white LEDs for data communication and lighting were employed as a means to demonstrate the feasibility of indoor optical data transmission with pioneering work by Tanaka et al.[5] at Keio University.

In recent years the uses of Light Emitting Diodes (LEDs) for lighting, indoor communications, positioning and sensing have grown [6]. visible light communication (VLC)based on light emitting diodes systems, which used for indoor and outdoor applications to perform wireless communications , offer a huge bandwidth compared

with the radio frequency (RF) bandwidth technologies [7]. MIMO Visual Light Communication (VLC) is now more popular due to its ability to transmit a very data rate. In a mobile environment allows concurrent data stream transfers through the use of multiple lighting units that are normally used for room illumination allowing for more data throughput[7]. As an indoor / outdoor wireless networking medium, OWC contains visible optical light (VL) and infra-red (IR) regions of spectrum. The OWC division is Visible Light Contact (VLC). The VL (390 nm-750 nm) band is working. The IM / DD approach is recognized as the very important modulation method for transmitting data using visible optical light. Dataset on minor differences in strength are stored in IM / DD. Photo sensors detect variations on the target and transform them into digital data[8].

VLC systems using LEDs and standard photodiodes (PDs) were used in many indoor applications with high data rates Rb over short ranges of Line of sight (LOS) communications. However, LOS-based connections have some limitations such as shadowing and restriction of user versatility. These disadvantages can be solved using: multi-array transmitters (Txs) and receivers (Rxs) and hence the system costs are raised. [9]. The general use of intelligent devices that compact with LED-based screen illumination, flashlight and quality cameras gives the possibility to create VLC connections, so that the flashlight and camera are used without external hardware as a transceiver. The OCC provides new working power for the use of VLC systems in a range of applications, including DST, D2DC, as part of the Internet of Things, for vehicle communications where Rx is based, including the vision, data transmission, location and scale of multiple operation [10].

1.2 VLC SYSTEMS

VLC systems introduced many advantages that can be used as indicators to show the benefits and importance of that systems.

1.2.1 Advantages of VLC Systems

Some of the compelling advantages of VLC technology are summarized below.

- **Broad bandwidth:** The EM spectrum optical band is orders of magnitude wider than the RF. In IR and VL bands alone the available bandwidth is around 2600 times the bandwidth of the RF band[11].

- **Simplicity and economic efficiency:** VLC use digital baseband technologies that simplify transmission and reception than RF communication where cohesive methods such as heterodyne reception add to the complexity of the system. In addition, VLC can be introduced using relatively cheap front-end devices including commercially available LEDs and PDs[12].
- **Energy efficiency:** Highly energy efficient optical sources, such as LEDs are available. Compared to traditional lights, LEDs need 80 percent less power. In addition, in VLC applications, the power used by LEDs is mainly used for illumination because the data transmission is piggy-backed by illumination. Moreover, energy efficient VLC techniques exist when lighting is not necessary, allowing data communication even when light is dark and off[13].
- **Security and spatial reuse:** Optical radiation does not penetrate opaque objects, as such it can be limited to well defined areas of coverage. This makes VLC an intrinsically protected media. Furthermore, the high level of spatial containment makes it possible for the VLC to coexist with proximal and non-interfering connections. This makes a higher density of data.
- **Avoidance of interference:** Optical signal does not interfere with RF signals, making them ideal as a complementary solution for RF as in the RF/OWC hybrid system. OWC is also resilient against EM interference and does not interfere with the functionality of sensitive electronic devices. The OWC, in particular VLC, is therefore safe for use in areas where RF, including aerospace, medical services and petrochemical installations, is prohibited[10].

1.2.2 VLC systems Challenges

Despite the above attractions, the VLC also has constraints that are important to its implementation, including:

- **Non-negative signal propagation:** By implementing the VLC via IM/DD, the modulative signal needs to be both real-power and non-negative because the channel input provides instantaneous optical power. This presents additional restrictions on the modulation techniques used in OWC, thus which restricts the usage of well-researched modulation formats in RF communication[14].
- **Transmitter bandwidth:** The limited bandwidth of high luminosity phosphorus-converted LEDs (pc-LEDs). Bandwidth approximately 2,5 MHz

for white-light response and 14 MHz for blue-light response limits the usable data rate in VLC in particular[15].

- **Mobility:** For VLC systems, the LOS connection is the best choice, providing a higher SNR, a low error and high data rates. However, LOS connections are susceptible to blockage and thus restrict mobility, especially indoors. Non-LOS (NLOS) connections are more resilient to block and can provide greater user mobility support but for high-speed applications, the data rate is decreased by path loss and dispersion caused by many routes[15].
- **Transmission distance:** For the OWC system that uses LEDs as an optical source, the transmission distance is reduced because the distance lighting is sharply decreased. While laser diodes LDs can be used as light sources for obtaining guided beams with limited power loss, their use, due to their high radiant power, is subject to stringent eye protection regulations.

1.2.3 VLC Areas of Application

The above features make VLC an appealing choice in many areas of use. An overview of some VLC use cases is given below:

- **smart lighting and wireless internet access:** Indoor VLC can be used in homes and workplaces to provide wireless networking. With control, data and multi point coordination realized using power-over-ethernet (PoE) technology, the lighting devices illumined the room can also serve as optic access points (APs)[16]. VL spectrum for downlink transmission to devices can be used during such deployment, while uplink transmission can be provided by IR spectrum[17]. Indoor VLC can also be used to deliver an intelligent lighting solution that tracks factors such as light intensity and color to adjust the light level in an area and saves power[18].
- **Indoor localization:** The growing number of the LED luminaires within a typical indoor building exploits the specific identification of each LED source to ensure higher exactness and resolutions of several centimeters in VLC-based positioning[19].
- **Communications in-flight:** In aircraft with unwanted use of RF radiation, LED-based lighting used in aircraft cabins are a possible VLC transmitter for both lighting and passenger communication services[20].

- **Communication with the vehicles:** LED traffic lamps, street light and car lights can be used to set up the VLC. Traffic lights and road safety notices can be sent to the driver. Cars can also interact in the same vein with one another with head and tail lights to avoid accidents[17].

The standard VLC device model is shown in Figure 1.1. The beam is modulated by amplitude and propagation by a free space channel (i.e. LOS, NLOS, etc.). On the Rx side the information is obtained and collected using an optical Rx to retrieve the transmitted data.

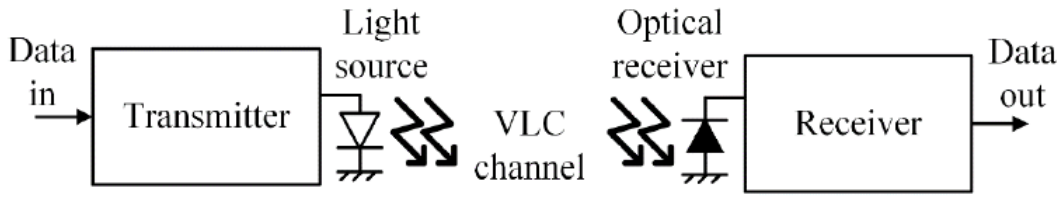

Figure 1.1: VLC block diagram

In VLC the light amplitude (i.e. the optical carrier signal) is emitted, and is unipolar and real-assessed.

1.3 THESIS OUT LINES

This thesis contains five chapters, chapter one includes an introduction about optical communication systems. Background of visible light communication systems is discussed in chapter two Chapter three covers NN and its application in communication systems while chapter three contains the proposed system details. Chapter four contains neural networks design and training for a specific VLC channel data and use the trained network in our system channel estimation. Finally, chapter five contains the conclusions and future works.

2. OPTICAL WIRELESS COMMUNICATIONS

This section explains the basic blocks of an VLC structure. Figure 2.1 displays the block diagram of a standard VLC system. An VLC system, which is common to every other system of communication, consists of three main blocks: the transmitter, the receiver and the channel. Each of these blocks is discussed further below.

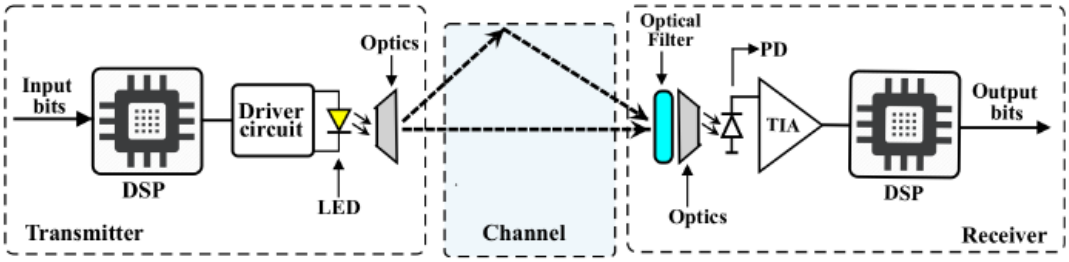

Figure 2.1: VLC system general block diagram

2.1 OPTICAL TRANSMITTER

The optical transmitter modulates data/information through intensity modulation (IM) on the optical carrier. This means that the light produced by the optical light source in accordance with the modulating information signal varies in power (intensity). The transmitter consists of a digital signal processor (DSP), which modulates the data bits digitally, and a digital to analog converter (DAC), which converts the DSP output into an analog modulating signal. A driver circuit is then used in proportion to the modulating signal to control the current flow through the optical source. The optical source transforms an optical power of the information-carrying current signal. An optical device consisting of a mirror, a collimator or a diffuser may then be used to pick up, focus or expand the optical beam to the recipient. LEDs (incoherent sources) and LDs (coherent sources) are the most frequently used optical sources. The choice of the optical source to be used will depend on the objective application. LED's normally emit a wider beam than LDs, the average LED spectral range is approx. 40 nm, and the LD's are approx. 1 nm[21]. LEDs are also used primarily for indoor applications. However, they can also be used for short-range outdoor VLC connections up to one kilometer. LDs are primarily used for VLC long-distance outdoor connections due to their highly directional beam profile that limits canal power loss. However, because of its high radiant strength they are subject to strict eye protection regulations[22]. For VLC, the

rate of intensity variation in the optical source is much faster than the human eye's response time, such that the light emitted is actually perceived as constant glow[23].

2.2 OPTICAL RECEIVER

The key function of the recipient is to extract the data from the light transmitted. Direct detection (DD) is used in which the PD generates an electric signal proportional to the immediate optical power obtained[12]. To absorb and focus incoming light to the PD, an optical system, e.g., collimator lenses are used. An optical filter may also be used to choose a portion of the optical spectrum (e.g., wavelength) and also to eliminate or reject the unwanted noise in an environment of light. APD or series of PDs then produces picture current, which is proportional to the optical power of the incident. A circuit for post-detection amplifies and filters signals in order to eliminate unwanted signals. This includes a transimpedance amplifier (TIA) that amplifies and transforms the PD photo current into a signal voltage. Finally, an analog to digital converter (ADC) is used to translate the signal from analog to digital, and the demodulation necessary to retrieve the transmitted information bits is performed by a DSP block. The two popular PD types are intrinsic (p-type and n-type) photodiode and avalanche photodiode (APD). The PIN PD is smaller than the APD, but its construction is simpler, cheaper and provides a greater active region. These features make PIN PDs the most used PD for VLC. Using DD on the receiver, transceiver devices without complex high-frequency circuit designs in coherent systems are easier and cheaper to deploy. However, the simplicity of DD implies that the frequency and phase information of the optical carrier is lost. The two main noise sources in the receptor include shooting noise in the obtained photo current generated by ambient lights such as the sun and other artificial lights and the thermal noise from the receiver electronics (e.g., amplifier). The shot and thermal noises called Gaussian noise[13].

2.3 OPTICAL WIRELESS CHANNEL

It should be stressed that OWC interconnection deficiencies will dramatically affect device efficiency and power. These deteriorations involve the interference caused to the received signal by the optical wireless channel. Therefore, to understand the characteristics of the optical wireless channel well is really necessary in order to plan, install and run an effective OWC device so that the effects of channel distortions are measured and controlled. The characteristics of OWC channels depend largely on the

communication surroundings, such as indoors, outdoors, underground and underwater[24]. In addition, environmental information influences the characteristics of the channel. For example, household or office buildings, warehouses, shopping centers, etc. indoor conditions are incredibly diverse. Therefore, diverse conditions induce various characteristics of the optical signal. Secondly, the optical transmitter OTx and optical receiver ORX's locations and their shared orientation towards reflecting surfaces. The implementation of indoor characterization technologies is not therefore very successful to evaluate the channel characteristics and the device efficiency of the outdoors (or underground and underwater)[24]. In comparison to RF, multi-path optical wireless link fades. This is the product of the millions of optical wavelengths that exist in DP dimensions in OWCs, resulting in a high degree of immunity to multisectoral decay that is powerful spatial diversity[22]. Thus, no small fading exists in the OWCs. In addition, IM / DD use eliminates local oscillators in the transmitter and receiver and thus no FOs in the OWCs. As far as Doppler is concerned. Article [25] shows that Doppler frequency in OWC systems has negligible results. The resulting change in the wavelength small enough such possible to suppose that bandwidth distribution and Doppler SNR differences are minor issues in the majority of IM / DD devices.

2.3.1 Channel Impulse Response (CIR)

This optical communication channel can be described as a linear system for the time invariance (LTI) with input amplitude x(t), output signal y(t)t and channel impulse response h(t)[26]. CIR h(t) is the signal in time domain obtained by the ORX if an OTx optical pulse is transmitted indefinitely short[27]. CIR h(t) helps you to estimate the time domain performance of the device. Until the CIR h(t) is known, a multi-path propagation distortion of any waveform can be estimated and an unspecified input performance expected without checking can be expected. Any optical wireless link can mathematically be expressed as an equivalent base band model[22].

$$y(t) = x(t) \otimes h(t) + n(t) \tag{2.1}$$

Where: $\otimes$ is convolution operator, $x(t)$ is transmitted signal, $n(t)$ is the noise signal and $y(t)$ is the received signal. Consequently, a specific channel model should be provided and its CIR defined in order to capture OWC Channel Features.

2.3.2 DC Gain of the Channel

The optical signals take several paths to a fixed or handheld ORx in non-direct line-of-sight NDLoS and non-direct NDNLoS setups. Due to reflections off environments, multi-path propagation occurs. Due to the difference in the propagation path length the signal received is a total of weighted and delaying copies of the signal transmission[28]. There is a so-called temporal dispersion, so the optical channel extends the broadcast signal over time. The root mean square RMS delay range of CIR h(t), can be quantified:

$$D_{rms} = \sqrt{\frac{\int_{-\infty}^{\infty}(t-\mu_\tau)^2 h^2(t)dt}{\int_{-\infty}^{\infty} h^2(t)dt}} \tag{2.2}$$

Where, time of propagation denoted by t and $\mu\tau$ is the mean path gain which is given by[29]:

$$\mu_\tau = \frac{\int_{-\infty}^{\infty} t\, h^2(t)dt}{\int_{-\infty}^{\infty} h^2(t)dt} \tag{2.3}$$

2.4 TECHNIQUES OF OPTICAL WIRELESS MODULATION

This section analyses OWC's optical modulation schemes. The emphasis is on modulation formats specific to the focus of this study. They include pulsing modulation systems including on-off-keying (OOK), PPM and PAM modulation, and multi-carrier techniques, particularly OFDM. As already mentioned, the modulated signal regulating the drive current in an IM/DD-based optical wireless device proportionally changes the strength of the optical source. The equivalent IM/DD device baseband model is expressed[12]:

$$r(t) = Rh(t) \otimes s(t) + \eta(t) \tag{2.6}$$

Where:

⊗: represents convolution.

s(t): optical source intensity.

r(t): photo current generated by the PD.

R: responsivity of the PD.

$\eta(t)$: amount of thermal noise and shot noise because of the ambient light. It can be modeled as AWGN with zero average and variance σ^2.

The channel input s(t) is a non-negative instantaneous optical power, as in equation (2.7)[12]. The average optical power transmitted is P_{ave} can be calculated as:

$$P_{ave} = \lim_{T\to\infty} \frac{1}{2T} \int_{-T}^{T} s(t)dt \tag{2.7}$$

where T is the transmitted light wave period. The relation between the average received optical power P_r to the average optical power is :

$$P_r = hP_{ave} \tag{2.8}$$

Where h represents the DC gain of the channel, that is given by :

$$h = \int_{-\infty}^{\infty} h(t)dt \tag{2.9}$$

Through restricting P_{ave}, eye protection criteria on optical sources can be met to the degree that the overall allowable radiant power level does not exceed.

The choice of modulation techniques for OWC systems plays a key role in deciding important device parameters, such as power and spectral efficiency, as well as minimum error. For energy-strict applications such as sensors and IoT systems, power efficient modulation schemes are considered while for applications with high speeds, such as video streaming through home/office internet connection, bandwidth efficiency are favored. Below is an additional discussion of common modulation schemes.

2.4.1 On-off-keying

Due to its simplicity, OOK is the simplest pulsed IM/DD system for optical communication. However, OOK transmits only one bit per symbol interval as a binary modulation device, thereby providing minimal spectral efficiency. OOK represents binary data in the form of high intensity (on) and low intensity (off) as its name implies. A high intensity is bit '1' and a lower intensity is bit '0.'[22]. OOK is typically implemented using the pulsed non-return (NRZ) format, where a pulse for the whole symbol length is transmitted T. However, the OOK can also be built with a pulse format of zero (RZ) by sending the optical pulse over a fraction of the symbol interval to give

an improved efficiency over NRZ-OOK, even when the bandwidth demand is increased. Figure 2.2 shows NRZ-OOK and RZ-OOK signals[30].

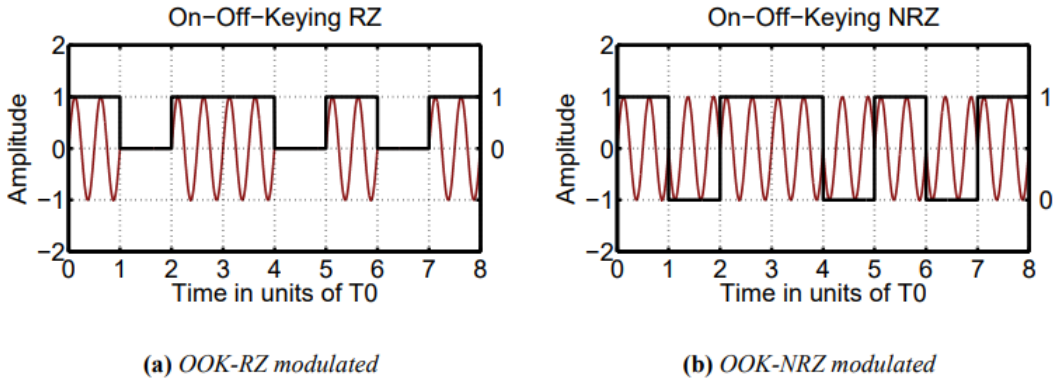

(a) *OOK-RZ modulated* **(b)** *OOK-NRZ modulated*

Figure 2.2: Optical modulation (a- RZ-OOK b- NRZ-OOK)

2.4.2 Pulse Amplitude Modulation

An L-ary PAM scheme transmits information using several levels of intensity where L indicates the magnitude of the signal constellation diagram, i.e. the amount of level of optical intensity. So, each PAM constellation transmitted by a symbol interval is mapped with $\log_2(L)$ bits. The non-negative restriction of optical signal transmission, unipolar L-PAM is used in OWC,and the intensity levels are given by[31] equation (2.10).

$$P_l^{PAM} = \frac{2P_{ave}}{L-1} \quad \{\text{for } l = 0,1,2,\ldots..L\text{-}1\} \tag{2.10}$$

Figure 2.3 contains 4-PAM optical modulated signal[32].

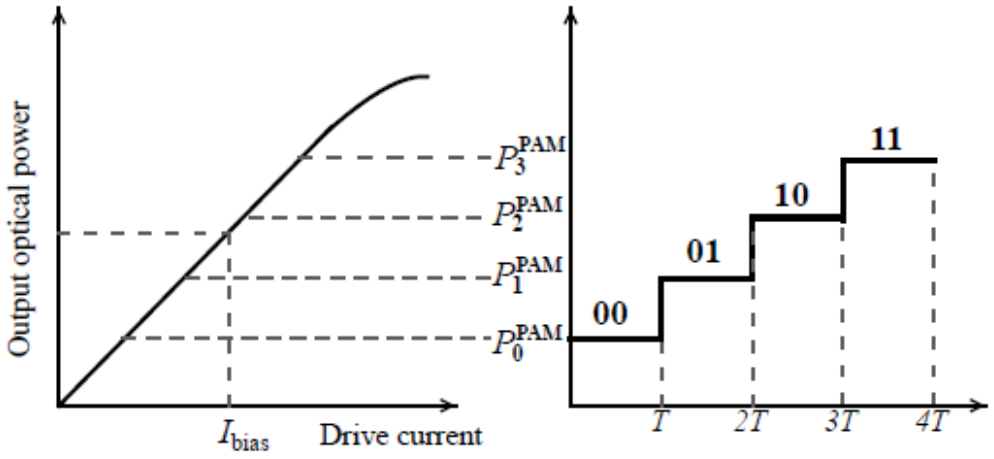

Figure 2.3: Optical 4-PAM signal.

2.4.3 Pulse Position Modulation

In the L-ary PPM, the duration of the symbol is split into subintervals/slots of L time, each with Tc = T= L duration. Data is transmitted by adjusting the time offset (position) of the optical pulse over the duration of each symbol. A filled time slot has a pulse intensity level of PPPM on while the rest of the empty slots (L-1) have a low intensity PPPM level. The signal constellation scale of a L-ary PPM system is L. The transmitted constellation (symbol) is indicated by the pulse location and the $\log_2(L)$ bits are mapped to the L constellations. As L increases, L PPM modulation increases its power efficiency and error performance. The average PPM power consumption is less than OOK and PAM. PPM has a shorter pulse interval, which means that it needs a higher bandwidth. As a consequence, PPM is less effective than PAM[33]. In order to increase spectral efficiency, different variants of PPM were proposed. For example Overlapping PPM (OPPM)[34] and Multi-pulse PPM (MPPM)[35]. 4-PPM optical signal illustrated in figure 2.4 [34].

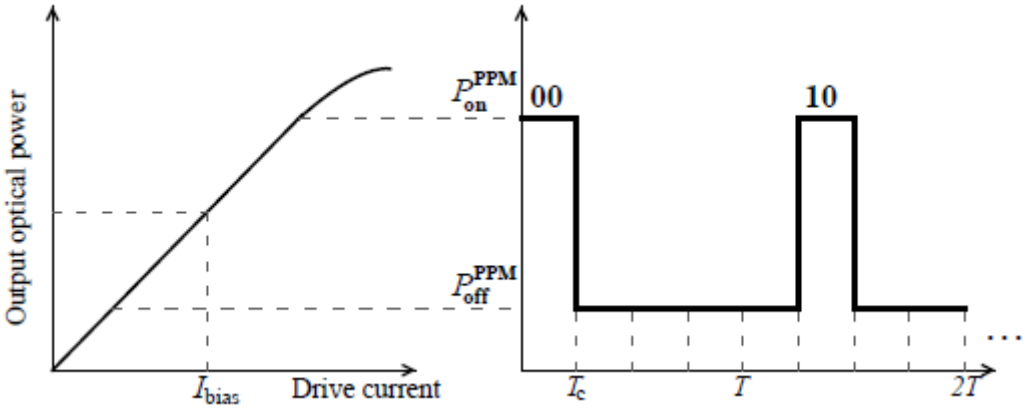

Figure 2.4: 4-PPM optical signal.

2.4.4 Optical Orthogonal Frequency Division Multiplexing OFDM

The increased frequency selectivity induced by the LED response and the multifaceted propagation of the transmitted signal contributes to ISI as transmission speed increases. The data rate that can be obtained from the above pulsed modulation techniques is limited by the presence of ISI. Multi-carrier modulation techniques like OFDM have therefore evolved to be the primary candidate for high data rate OWC systems. OFDM is a bandwidth-efficient transmission technology[36]. In OFDM, a wideband channel is subdivided into many narrow bands and orthogonal subchannels used to concurrently transmit separate data streams. Each sub-channel is referred to as a sub-carrier (SC). Usually, a conventional modulation scheme, AM, is employed to modulate information on each SC. The system blocks for the optical OFDM are shown in Figure 2.5. The data bits are mapped to constellations of QAM symbols. The QAM symbol stream is then transformed to a parallel using serial-to-parallel (S/P) block of symbols, allocated to the SC in each OFDM frame. The multiplexing of parallel streams requires an inverse fast Fourier transform (IFFT) operation and generates an OFDM time domain signal[36].

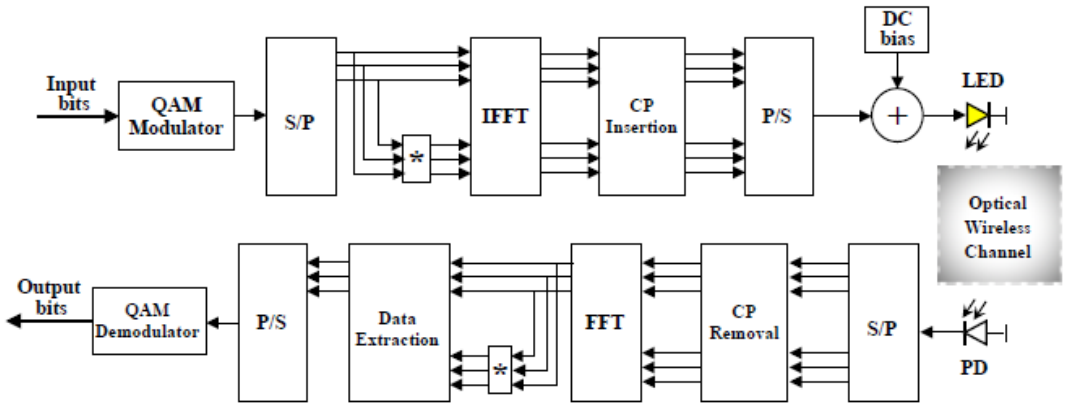

Figure 2.5: Optical OFDM system block diagram

2.5 OPTICAL MIMO TECHNIQUES

The use of multiple elements in MIMO systems by the transmitter and receiver is essential technology to improve wireless communication capability and/or reliability. In RF-based communications systems, techniques for the multiplexing gain, diversity gain, or antenna gain were thoroughly explored and implemented to improve the bit rate, error, or signal-to-noise interface ratio of wireless systems, respectively[37]. MIMO techniques were also proposed for OWC systems inspired by the performance achieved in RF systems. An optical transmitter may use a range of optical sources that can be configured for the transmission of MIMO data. Optical MIMO technology is designed to take advantage of additional freedom, such as the position and viewing angle of the optical sources, and the optical detectors' place[38]. These technologies are promising solutions that allow effective use of available bandwidth at data rates and increase communication device coverage and reliability. In order to insert channel signatures (signal strengths) on multiple connections, MIMO techniques use the wireless channel. These signatures allow the recipient to differentiate the signals from various transmitter sources. Figure 2.6 shows a simplified schematic of a MIMO system for OWC[38].

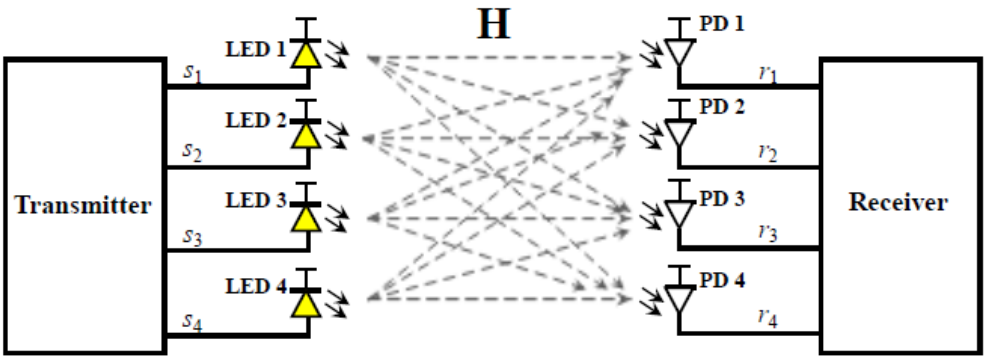

Figure 2.6: MIMO optical communication system.

For OWC indoor and outdoor environments different MIMO strategies have been proposed, each with its own unique features and advantages. In outdoor FSO systems, the MIMO system is used to boost system efficiency by spatially segregated optical wireless channels with LOS lineup. FSO systems are investigated in[39] using MIMO diversity technology to counteract the effects of turbulence-induced fading with redundancy.

2.6 MEASUREMENTSs AND MODELING OF MIMO VLC CHANNEL

MIMO VLC is a good technology for future OWC networks. This technology has drawn the interest of researchers because it aims to increase connection Robustness and high spectral performance (more bits /s/Hz) dramatically in comparison with IR LAN [40]. Figure 2.7 shows the propagation model for VLC channel, which include LOS and non-LOS propagations [41].

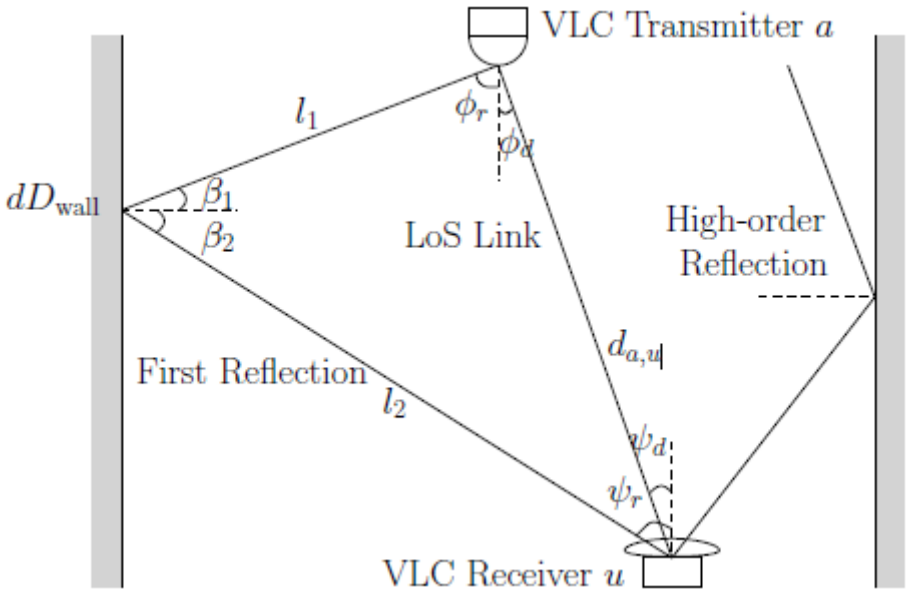

Figure 2.7: VLC propagations

The monochromatic diagram of VLC partnerships, like the line of sight (LOS), the first reflection and reflections in the high order., as seen in Figure 2.7. However, according to all connections, the total optical ability that is shown more than once is insignificant and neglected according to[42]. Model showed in Figure 1, contains a VLC transmitter installed on the room top transmits light to a VLC detector receiver. The irradiance angles for the LoS propagation and the first-reflected propagation are denoted as $\emptyset_d$ and $\emptyset_r$, while the incidence angles in each connection are indicated as φ_d and φ_r, respectively. The total DC attenuation from the transmitter to receiver link can be expressed as in equation 2.11 [43]:

$$h_d[u,a] = \begin{cases} \frac{(w+1).A_{PD}}{2\pi d_{a,u}^2} \times cos^w(\emptyset_d) \times T_s(\varphi_d) \times g(\varphi_d) \times cos(\varphi_d) & \text{for}(\varphi_d > \varphi_F) \\ 0 & for(\varphi_d < \varphi_F) \end{cases} \quad (2.11)$$

In some of the specific VLC channel features important research has been devoted for modeling the VLC interface. The effect of the multi-path propagation exerted by a reflection may in particular be studied with a multi-path power distribution profile (PDP) which is used to transmit the signal received. Lee et al. suggested one of the frequently used VLC networks, which includes multi-channel PDP[44].

$$h(t) = \sum_{n=1}^{N_{LED}} \sum_{k=0}^{\infty} h^{(k)}(t; P_n) \quad (2.12)$$

2.7 CHANNEL ESTIMATION METHODS

The LS channel estimator and the MMSE channel estimator are two principal pilot channel techniques. Estimators are referred to as one-dimensional (1D) estimates, i.e. a single-dimensional calculation of training sequences and NP length, whether in the frequency or time domain. They are widely used for estimating pilot-based networks because of their flexibility[45].

2.7.1 Least-Squares Method Based Channel Estimation

The estimator of the LS channel minimizes the squared error between the received signal and the transmitted signal. This estimate process is described by Equation 2.13.

$$\hbar^{LS} = arg_{\hbar^{LS}} min\|y - \hbar^{LS}S\|^2 \tag{2.13}$$

where $\boldsymbol{S}$ ($\boldsymbol{S}\epsilon\mathbb{C}^{NT\times NP}$) is the matrix for the transmitted data sequences and training data $\boldsymbol{s}nt$ (nt=1,2,…,NT) of all transmitters as explained in equation 2.14:

$$S = \begin{bmatrix} S_1 \\ S_2 \\ . \\ . \\ S_{N_T} \end{bmatrix} \tag{2.14}$$

The channel estimation between the transmitter antennas and the n-th receiving antenna is given by:

$$\hat{\boldsymbol{h}}_n^{LS} = \boldsymbol{y}_n \boldsymbol{S}^H [\boldsymbol{S}\boldsymbol{S}^H]^{-1} \tag{2.15}$$

2.7.2 Channel Estimation by Means Minimum Mean-Square Error Method

The MMSE principles that constitute a more detailed LS channel calculation are illustrated in Figure 2.8[46].

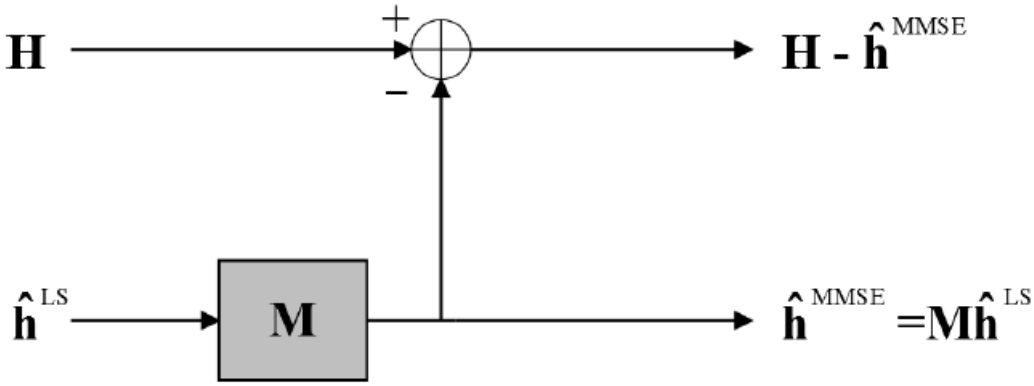

Figure 2.8: MMSE channel estimation block digram

The approach based on the MMSE channel estimate minimizes the MSE in the right way, $\boldsymbol{H}$, and the MMSE estimated channel, $\boldsymbol{h}^{MMSE}$, by having a strong linear estimation in terms of $\boldsymbol{M}$ and the optimum value of LS estimate, $\boldsymbol{h}^{LS}$:

$$\boldsymbol{h}^{MMSE}=\arg \hat{\boldsymbol{h}}^{MMSE}\min||\mathrm{H}-\tilde{\boldsymbol{h}}^{MMSE}||^2 \tag{2.16}$$

Because the MMSE assessment focuses on MSE reduction, it does better than the LS channel estimation. The drawback is that it is focused on channel statistics. This method is more difficult than the LS estimator. The technique for reducing the complexity of the MMSE estimator is suggested in the MMSE adapted channel [46].

2.7.3 Chanel Estimation Based on Neural Network

The Acceptable channel state information (CSI), by rudimentary calculation methods and an appropriate number of pilots, was and remains of major importance in mobile communication systems. This is very difficult, particularly for high-dimensional signals in time, frequency and space. For example, with the very complex LS estimator, it is often difficult to achieve adequate efficiency, whereas the minimum mean MMSE is complex and can hardly be achieved. Given the recent results of profound research for hard identification and calculations, the significant advantage of the functional channel estimator with complications (near) LS calculated and (near) MMSE estimates, it seems very important to try to test the channel in relation to deep neural networks (DNN)[47]. For large data sets to be trained[48], traditional DNNs need several parameters. This collection of data is correlated with the few symbols that were obtained from the DNN-based signal pilot, indicating that a number of pilots have to be accurately measured using DNNs. This refers in particular to large-scale MIMO-OFDM signals. Given the recent development of the advanced technologies, although the computational

complexity of DNNs is fair, pilot symbols need maximum bandwidth and should be retained as low as possible. The DNN training demand for data therefore represents the main obstacle for estimating channels to the use of data [49].

2.7.4 Linear Regression

Linear regression is an approach used for matching a linear equation with measurement data to form the relationship between two variables. One variable is known as an explanatory variable and the other as a dependent variable. One modeling system may like, for example, a linear regression model to connect the weights of individuals with their heights. A model should first assess if the variables of significance are related to or are not related to the observed information until the attempt to adapt a linear model. This does not necessarily mean that one variable affects the other, but that the two variables are substantially related. A dispersal can be a helpful method to assess the force of the relationship between two variables. If the proposed explanatory variables and dependent do not appear to be related to them, it is possible that the useful model will not be fitted in with a linear regression model. The coefficient of correlation, which shows the frequency of the interaction of the observed figures for the two variables, is a valuable numerical indicator for the association of two variables. The general equation of linear regression algorithm is[50]:

$$Y = a + bX \tag{2.17}$$

where X is the explanatory variable and Y is the dependent variable. The slope of the line is b, and a is the intercept (the value of y when x = 0).

3. NUERAL NETWORKS

3.1 ARTIFICIAL NEURAL NETWORK

An artificial neural network is a computational model inspired by the real brain of living organisms and its biological processing of information. It belongs to the group of artificial intelligence. It is used where we do not know the exact mathematical description between input and output. Scientists have in the past been inspired by the simplicity of the insect brain due to its complex functions. Although the insect's brain weighs fractions of a gram, it is able to provide flying, orientation, adaptation to wind changes or even predator detection[51].

3.2 NEURON

A neuron is a nerve cell that transmits and processes information from the environment and thus determines the body's ability to respond to these stimuli. A neuron generates electrical impulses that are transmitted from axons through synaptic gates to dendrites of other neurons. Axons and dendrites are protrusions of neurons that divert and receive information[52]. The intensity of the transmitted pulse affects the behavior of other neurons. These neurons, after exceeding a certain threshold, themselves create an impulse and thus ensure the transmission of information in the brain tissue. Synaptic transmittance changes after each signal pass. This phenomenon ensures the memory capacity of neurons. During learning, new memory paths are created and reminders disappear[53].

3.3 ARTIFICIAL NEURON

An artificial neuron (hereinafter referred to as a neuron) can be considered as a mathematical function of the inputs x and the output y. Inputs model dendrites and can take real values. In a neuron, they are multiplied by synaptic weights w, expressing their permeability. As with a biological neuron, an artificial neuron has an activating function at the output that has the status of a neuron as input. When the threshold value is reached, the activation function starts and sends a pulse. Synaptic scales play a role here in memory and are one of the main parameters in learning the neural network. The higher the weight value relative to other input weights, the more it affects the internal state of the neuron. Activation functions also contain so-called bias. This parameter

expresses the susceptibility of the activation function to switching. Figure 3.1 shows simple artificial neuron model[53].

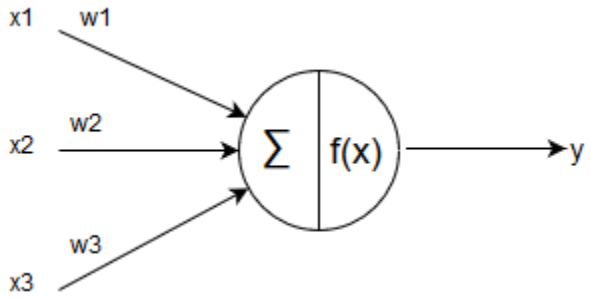

Figure 3.1: Artificial neuron model

A neuron with N inputs can be expressed mathematically as:

$$y = f(\sum_{n=0}^{N}(w_n x_n)) \tag{3.1}$$

where f (x) is the chosen activation function, wn define the weights and xn neuron inputs. This type of artificial neuron is called the perceptron. The flow of information goes from input to output, so it belongs to the group of forward networks. Perceptron was discovered in 1957 by Frank Rosenblatt[54]. By configuring the scales and the type of activation function, this model is able to distinguish groups.

This mathematical model can be classified into two classes, for example, to perform the basic logical operators OR, AND or NOT. It divides the state space into two parts, which determine how the neuron decides. The decision level of the AND function can be represented by a straight line. On the x-axis the inputs are x1 and the inputs x2 on the y-axis we have any value below the line is evaluated at the output as 0 and above the line as in figure 3.2[53].

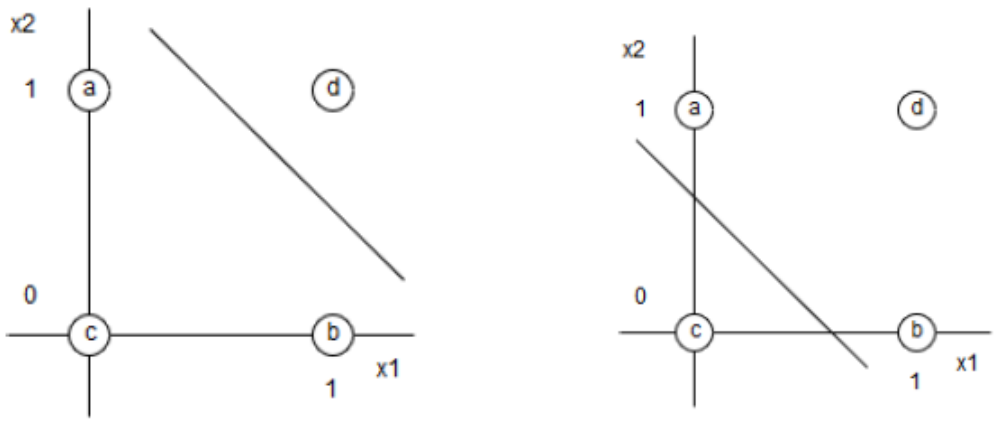

Figure 3.2: AND (left) and OR (right) functions.

The problem occurs if we want to teach this neuron the function of XOR, it requires dividing the area into other parts. The XOR operation requires 2 input values x1 and x2. If one of the values at the input is equal to one, the output of this operation will be exactly the value 1. This operation needs three decision stages, so we cannot create it with one neuron, which provides only two. One perceptron cannot map any function, so we use more neurons connected together, forming a network together. If we add more perceptions in a row, we have a multilayer network, figure 3.3. Neurons whose inputs are connected to previous neurons fall into the so-called hidden group. A deep neural network is then any network that has at least one hidden layer. The learning process of this structure is called Deep Learning[53].

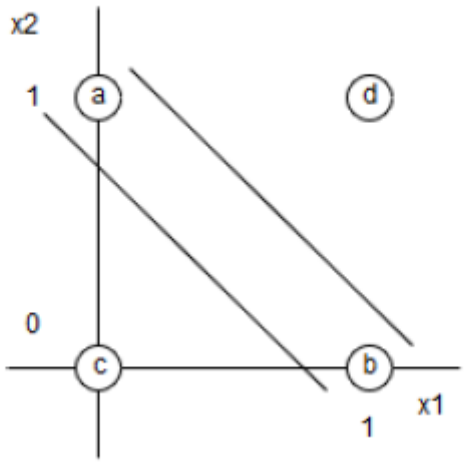

Figure 3.3: XOR function

3.4 NEURAL NETWORK ARCHITECTURE

3.4.1 Batch Normalization

This is a layer of the neural network that involves a change in the distribution of input values. In the context of deep learning, we mainly deal with the change in the distribution of inputs of internal nodes. The neural network changes the weights of each layer during training. This means that it also changes the activation of each layer. Because the activation of the previous layer affects the next layers, each layer in the neural network is confronted with a situation where the input distribution changes with each step. This is problematic because it forces each interlayer to constantly adapt to

changing inputs. During learning occurs changes in the distribution function of the input data, which makes learning more difficult. By applying this layer, we achieve the transformation of the inputs to the mean value of 0 and the variance of 1. This allegedly allows each layer to learn a more stable distribution of inputs, thus speeding up the learning of the network[55].

- **Dropout**
- Randomly chosen neurons are overlooked in this layer during exercises. They are tossed out unintentionally. This means their input to other neurons is eliminated momentarily in the forward section of the neuron and there are no weight updates in the reverse section of the neuron (learning). If a neural network knows, it settles in the network. Neuronal scales are tailored to particular specialized roles. Neighboring neurons depend on this specialization, which may contribute to an overly complex and training-specific model. It is possible for other neurons to join and learn the representation required to predict missing neurons if neurons are unintentionally knocked out of the network during training. This is expected to result in the network being taught more autonomous internal representations. The network is also less susceptible to the neuronal particular severity. This layer makes the network more widespread.[56].
- **Leaky ReLU**

  This is a modified activation function based on another activation function called ReLU (rectified linear unit). It performs the function f (x) = max (0, x). It is often used in neural networks because it has been found to significantly accelerate stochastic gradient convergence compared to sigmoidal or tanh functions [57]. ReLUs may sadly stop working Unfortunately. For example, a wide gradient that flows through a ReLU neuron can allow the weight to be upgraded to prevent the neuron from being reactivated. If so the gradient through the unit from that point on will still be null and empty. Leaky ReLU (Leaky Rectified Linear Unit) is one way to fix this problem. Instead of the max (0, x) function, which is zero when x <0, Leaky ReLU will instead have a small negative slope see figure 3.4[57].

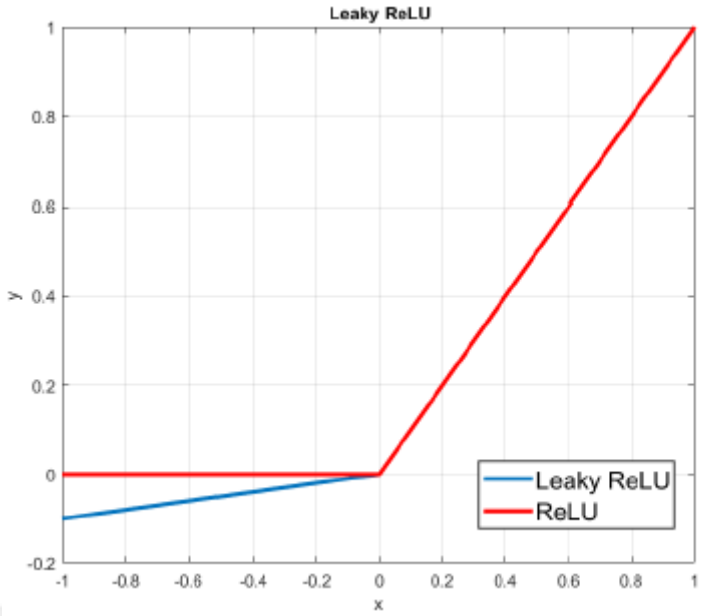

Figure 3.4: Responses of ReLU and Leaky ReLU functions.

- **Epoch**

  An epoch is a value describing the duration of the propagation of a sample of data from input to output and one step of learning.

3.4.2 Reverse Promotion

Back propagation is an algorithm for learning artificial neural networks. When designing a neural network, scales are initially initialized, usually with random values with a given distribution. When the input data is then propagated by the neural network, a result is obtained that differs from the desired values. To quantify a neural network error, they usually use error functions, such as the MSE (Mean Square Error) type. The backpropagation algorithm looks for the minimum value of the error function in space using a technique called a descending gradient. These weights are then changed in such a way as to reduce the overall error function. This process is called neural network learning. This is the expression $\partial C/\partial w$, where the partial derivative of the error function C is calculated with respect to any weight or bias in the network. This expression indicates the change in the value of the error function relative to the change in the weight value or bias values. Assume a neural network containing three input neurons, one hidden layer with the same number of artificial neurons, and an output layer also with three neurons. The mean standard deviation is selected as the error function. This network explained in figure 3.5[57].

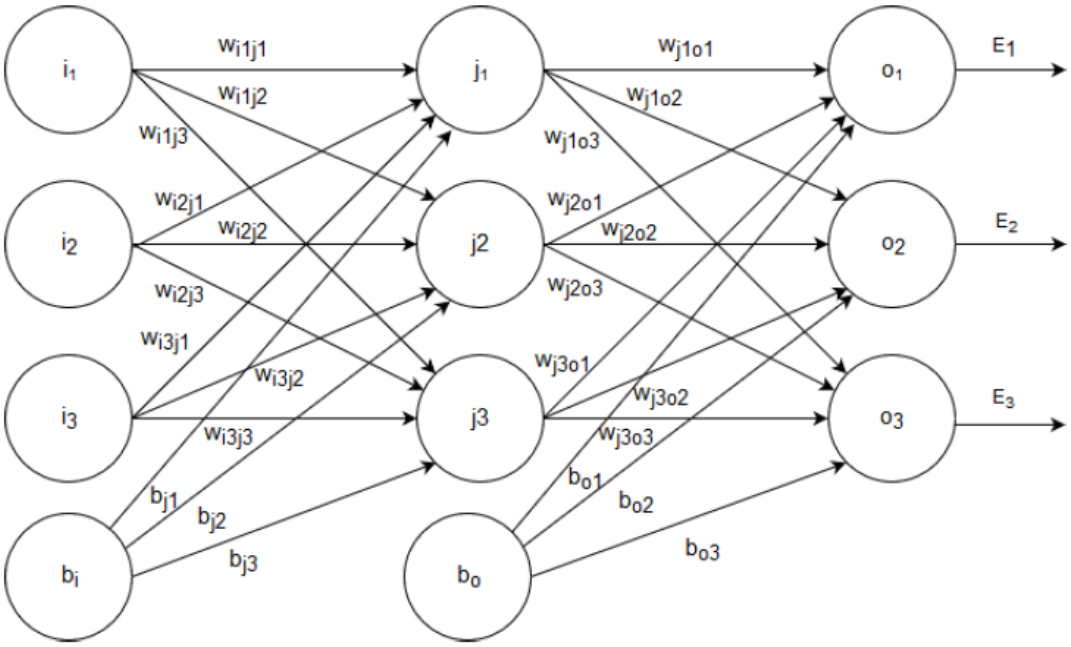

Figure 3.5: Weights and biases in a neural network.

The input vector of a neural network:

$[i_1\ i_2\ i_3]$.

and required output:

$[o_1\ o_2\ o_3]$.

The initial values of the scales are:

$$w_{ij} = \begin{Bmatrix} w_{i1j1}\ w_{i1j2}\ w_{i1j3} \\ w_{i2j1}\ w_{i2j2}\ w_{i2j3} \\ w_{i3j1}\ w_{i3j2}\ w_{i3j3} \end{Bmatrix} \tag{3.2}$$

$$w_{jo} = \begin{Bmatrix} w_{j1o1}\ w_{j1o2}\ w_{j1o3} \\ w_{j2o1}\ w_{j2o2}\ w_{j2o3} \\ w_{j3o1}\ w_{j3o2}\ w_{j3o3} \end{Bmatrix} \tag{3.3}$$

The initial values of the bias values are:

$[bj1\ bj2\ bj3]$,

$[bo1\ bo2\ bo3]$.

The propagation from the input layer to the following layer proceeds as follows:

$$[i_1\ i_2\ i_3]\begin{bmatrix} w_{i1j1} & w_{i1j2} & w_{i1j3} \\ w_{i2j1} & w_{i2j2} & w_{i2j3} \\ w_{i3j1} & w_{i3j2} & w_{i3j3} \end{bmatrix} + [b_1\ b_2\ ib_3] = [h_{in1}\ h_{in2}\ h_{in3}] \quad (3.4)$$

This is a matrix multiplication of the input vector and the weight matrix. Finally, the bias value is added[57].

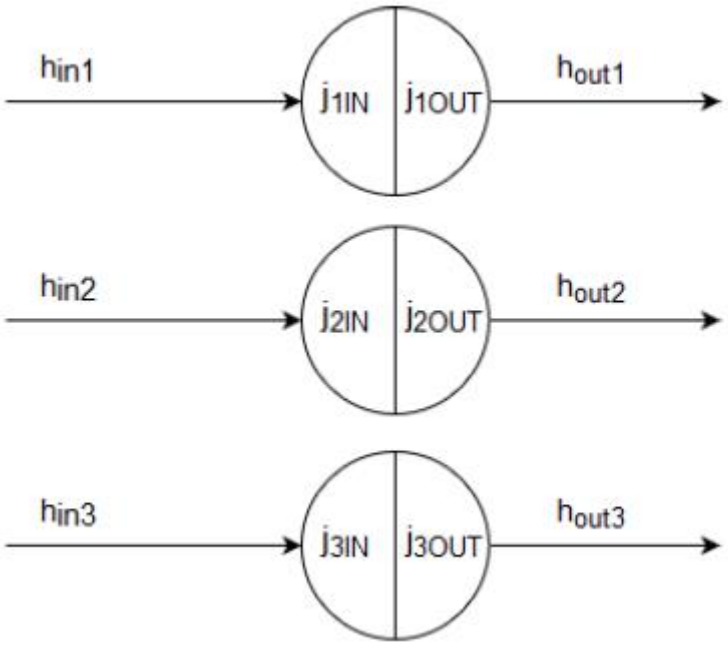

Figure 3.6: Hidden layers

3.4.3 Activation Functions

The values of h_{in} are the inputs of neurons in the hidden layer, in order to propagate the signal, it is necessary to apply an activation function to these inputs. There are many types of these functions, in this example the so-called Sigmoid will be described:

The sigmoid function has an output in the range (0, 1), which is ideal for binary classification problems where it is necessary to find the probability of data belonging to a certain class. This function is also differentiable at each point and its derivative is based on f '(x) = f (x) * (1 -f (x)). Because the term includes the same function, its value can be reused, which is an advantage in back promotions. Figures 3.7& 3.8 show both sigmoid function and its derivative respectively[58].

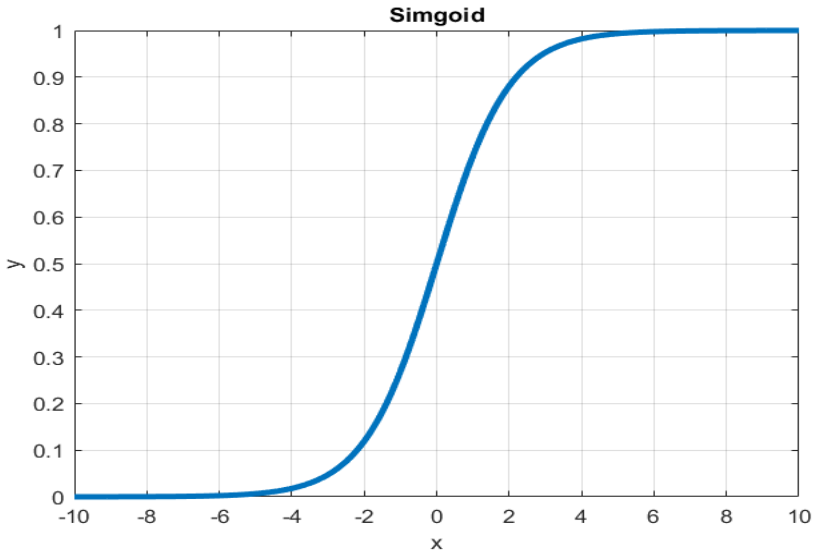

Figure 3.7: Sigmoid function

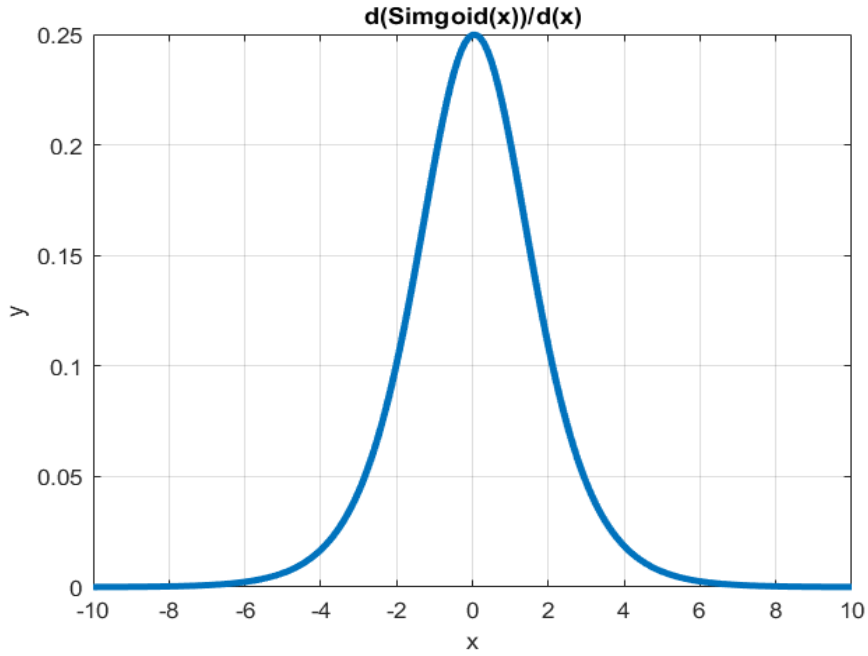

Figure 3.8: Sigmoid function derivative

Write function as :

$$\sigma(t) = \frac{1}{1+e^{-t}} \tag{3.5}$$

$$\sigma'(t) = \sigma(t) \times (1 - \sigma(t)) \tag{3.6}$$

Function application:

$$[h_{o1}\ h_{o2}\ h_{o3}] = [\sigma(h_{in1})\ \sigma(h_{in2})\ \sigma(h_{in3})] \tag{3.7}$$

These values then become output figure 3.6 and will be propagated to the next layer:

$$[h_{out1}\ h_{out2}\ h_{out3}]\begin{bmatrix} w_{j1o1} & w_{j1o2} & w_{j1o3} \\ w_{j2o1} & w_{j2o2} & w_{j2o1} \\ w_{j3o1} & w_{j3o2} & w_{j3o3} \end{bmatrix} + [b_{o1}\ b_{o2}\ b_{o3}] = [o_{in1}\ o_{in2}\ o_{in3}] \quad (3.8)$$

Again, application activation function:

$$[o_{out1}\ o_{out2}\ o_{out3}] = [\sigma(o_{in1})\ \sigma(o_{in2})\ \sigma(o_{in3})] \quad (3.9)$$

These values are the output of the neural network, which usually do not match the required values at the output, so it is necessary to train this network. Needed calculate the error function that will be minimized.

3.5 NEURAL NETWORK LAYERS

Neural networks consist of layers translated by multiple functions to convert the input signal to another one. The three main layer groups in a conventional neural network are convolution layer, pooling layer, and fully connected layer[59].

3.5.1 Pooling Layer

The pooling layer carries out a sampling process in order to combine (semantically) related features from the coevolutionary layer into one. A computer in a pooling layer takes the local patch as an input from an earlier function map (coevolutionary layer) and calculates the max. or average value for the patch. This decreases the representation dimension by reducing the number of parameters available in subsequent layers and increases the robustness of representations by invariance of minor variations and distortions[62].

3.5.2 Fully Connected Layer

Units in this layer are completely connected to all units in the previous layer, as seen in figure 3.1[63].

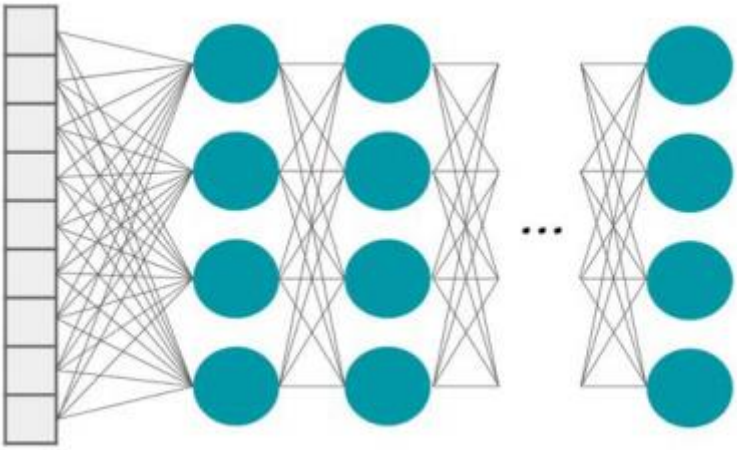

Figure 3.9: Fully connected layers

3.5.3 Classification Layer

This layer determines how the prediction score is determined using all previous layer outputs. Using the SoftMax classifier or the linear vector support machine to implement standard classification layers[64].

4. RESULTS AND DISCUSSION

The proposed method based on training a neural network with VLC system parameters (number of transmitters and receivers, room dimensions, optical devices positions, LEDs transmitted power, PD sensitivity), train the neural network using precalculated channel data, verified the trained NN, and finally apply the NN on specific VLC system data and obtain the VLC channel. To exam the NN performance the results compared with known channel. Figure 4.1 shows the proposed NN model. Linear regression method used for checking proposed NN algorithm performance. Table 1 contains the proposed system specifications.

Table 4.1: Proposed system specifications.

Item	Tx No.	Rx No.	MIMO Size	Data size (bit)	Room dim.(m)	Tx angle	Modulation	SNR dB
Spec.	4	4	4×4	4×16004	4×4×3	20˚	OOK	≤25
Item	Tx-Tx distance	Rx-Rx distance	Led color	LoS	Non - LoS	FOV	LED-height	n_floor
Spec.	0 – 4 m	0 – 4 m	White	Yes	No	0.349	1.48 m	0.15
Item	n_wall	n_ceiling	Channel size					
Spec.	0.7	0.8	4×4					

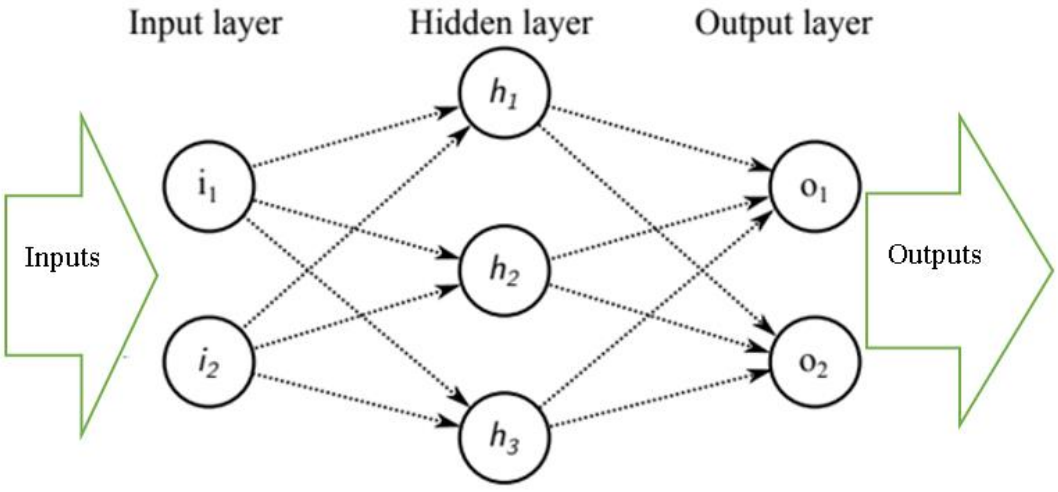

Figure 4.1: NN channel estimater

The proposed NN channel estimator performances shown in figure 4.2.

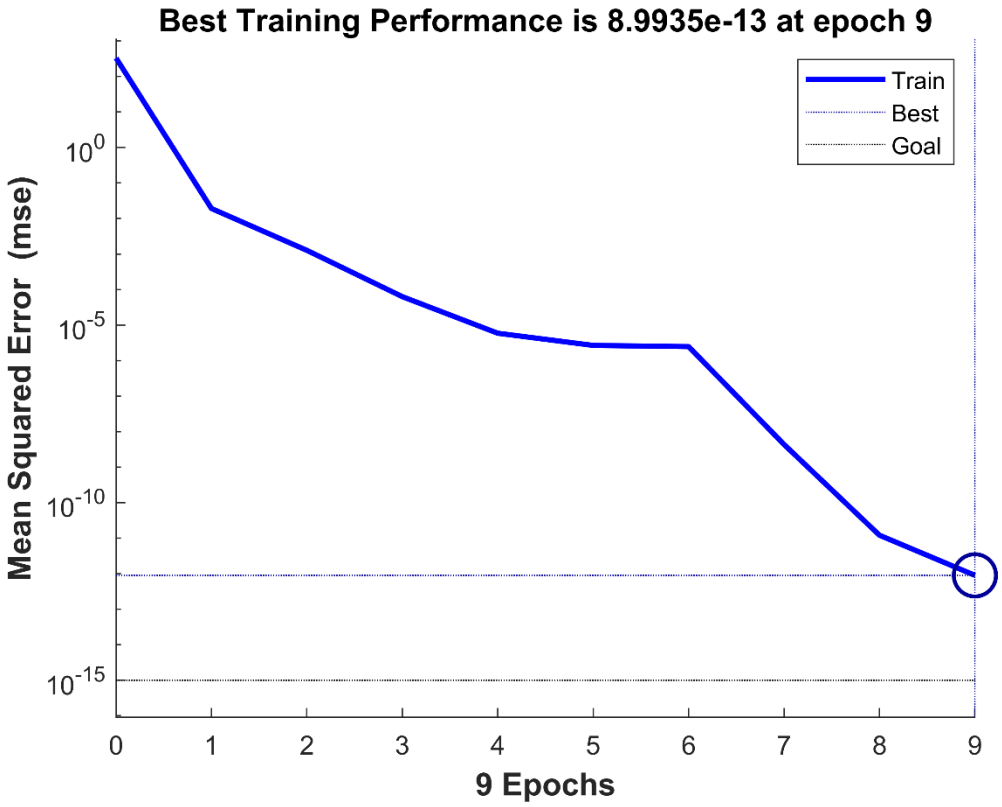

Figure 4.2: NN training performance

For the linear regression method, the mean square error is shown in figure 4.3.

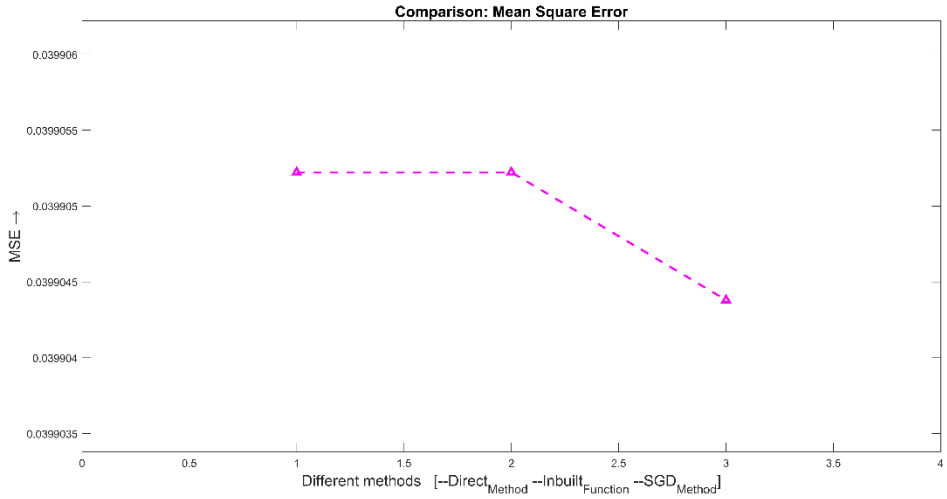

Figure 4.3: MSE for linear regression method

Figure 4.4 shows the BER for the proposed channel estimation algorithm in case of SNR =20 compared with theoretical BER. While figure 4.5 shows the BER for the proposed channel estimation algorithm in case of SNR =25 compared with theoretical BER

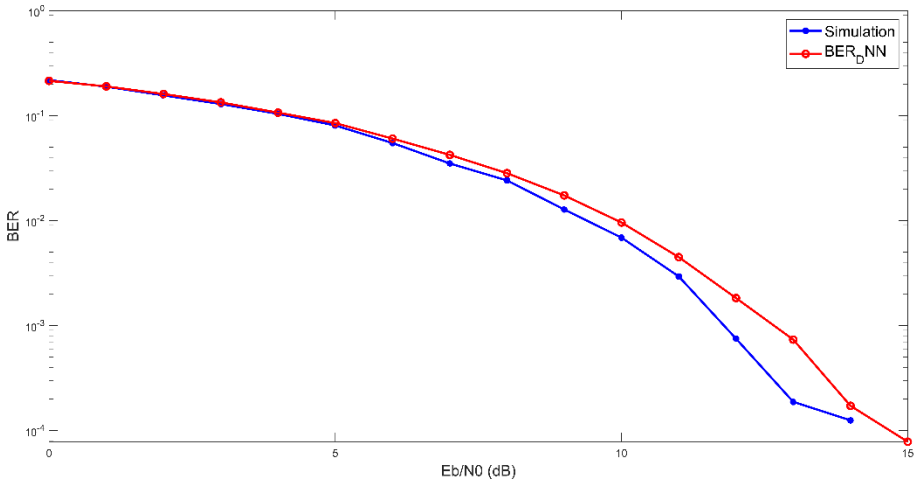

Figure 4.4: BER in case SNR=20

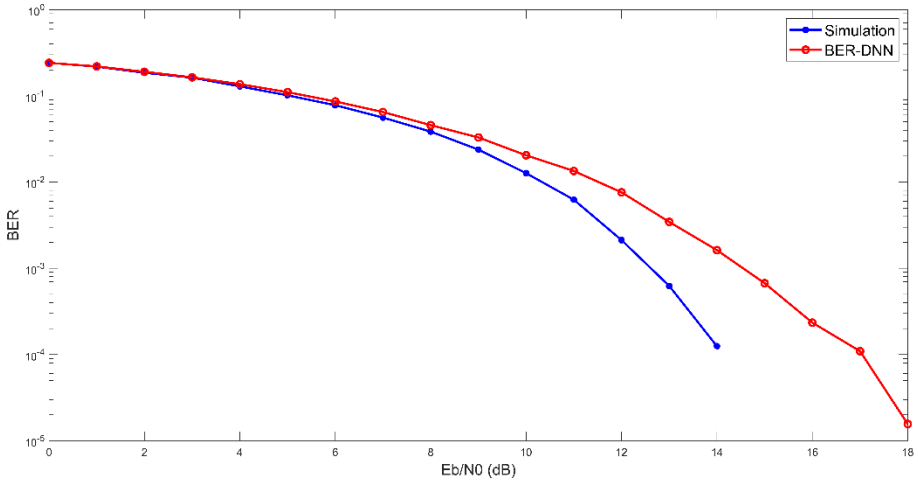

Figure 4.5: BER in case SNR=25

To satisfy the proposed NN estimation algorithm, the results compared with linear regression method. For linear regression method the linearity was done between the transmitted data and received data by NN.

The direct method linear regression is shown in figure 4.6. The results of using Stochastic Gradient Descent method is shown in figure 4.7, inbuilt MATLAB function linear regression results are shown in figure 4.8, while figure 4.9 shows the comparison between the used methods for linear regression and NN algorithm SNR.

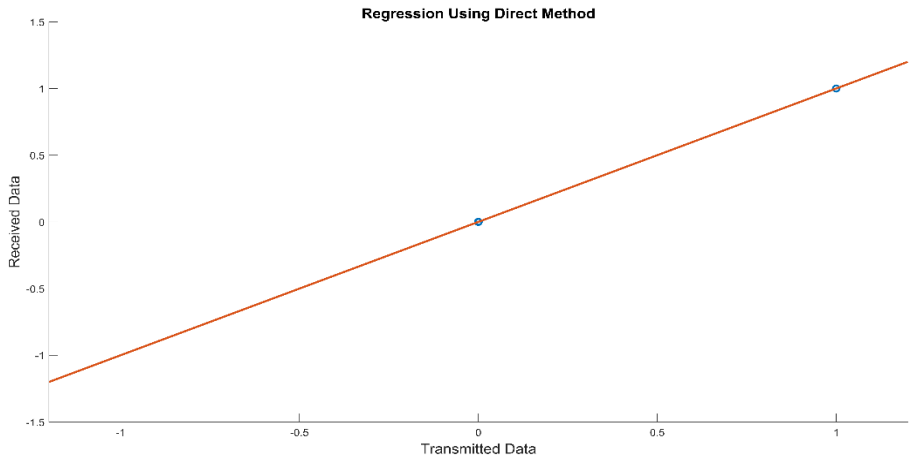

Figure 4.6: Linear regression using direct method

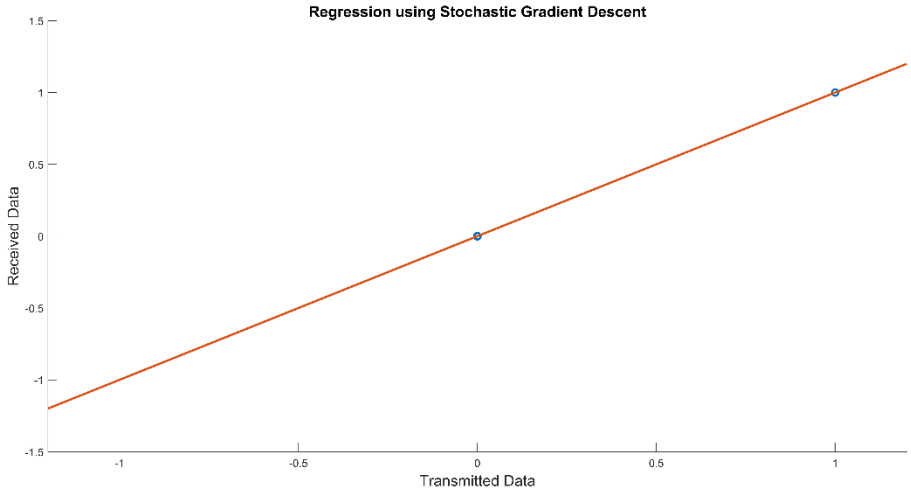

Figure 4.7: Stochastic Gradient Descent method

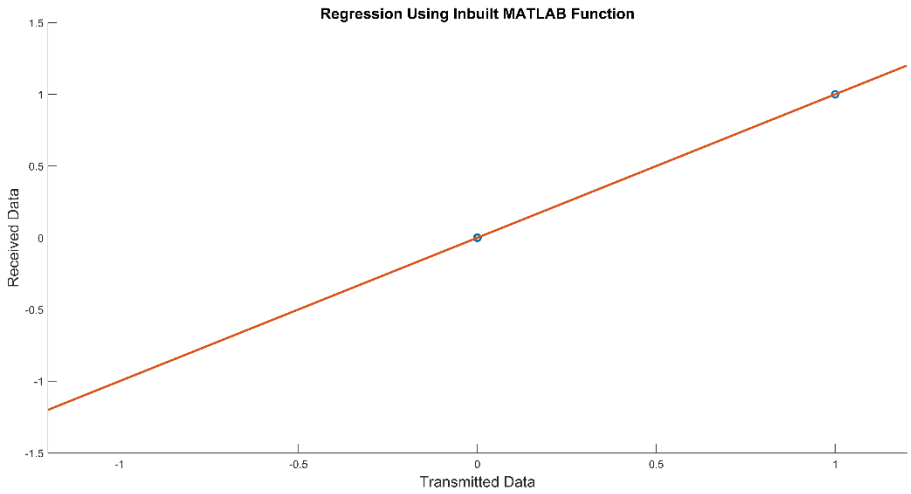

Figure 4.8: Regression Using Inbuilt MATLAB Function

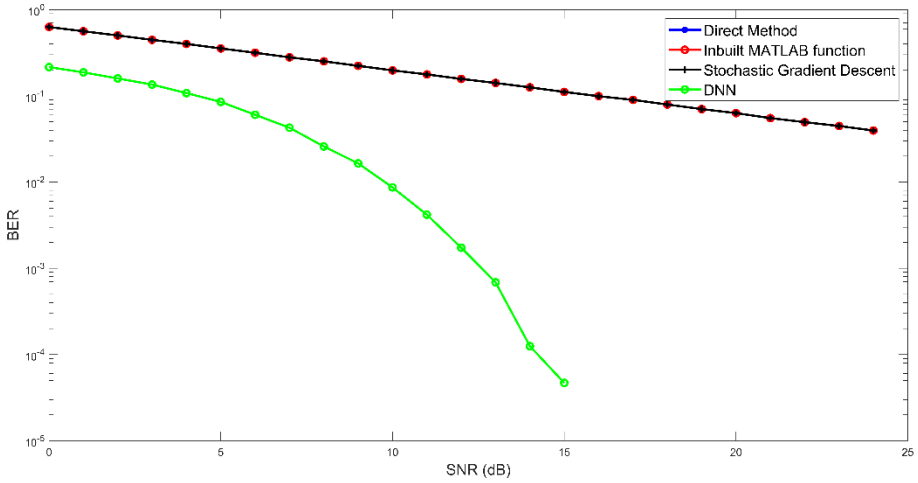

Figure 4.9: Comparing BER for both NN and linear regression

The comparison of BER shows that the NN based channel estimation method is best that the linear regression methods. It is clear that BER for the proposed method decreased with increasing of SNR and reaches a limit less than 10^{-4} while linear regression BER within 10^{-2}. BER for both proposed algorithm and linear regression method with respect to SNR are listed in table 4.2, while the MSE for both algorithms are listed in table 4.3.

Table 4.2: BER for both NN and Linear Regression w.r.t SNR

SNR	2	4	6	8	10	12	14	16	18
BER-NN	0.186	0.1	0.06	0.026	0.008	0.001	1×10^{-4}	1.5×10^{-4}	0.25×10^{-4}
BER-LR	0.469	0.396	0.365	0.251	0.197	0.158	0.126	0.1	0.079

Table 4.3: MSE for both NN and LR w.r.t SNR

SNR	2	4	6	8	10	12	14	16	18
NN-MSE	0.159	0.107	0.060	0.025	0.008	0.0017	0.0001	0.0	0.0
LR-MSE	0.504	0.399	0.314	0.25	0.198	0.158	0.127	0.1	0.08

5. CONCLUSIONS AND FUTURE WORK

5.1 CONCLUSIONS

This study, presented Channel estimation NN-based algorithm for MIMO VLC systems. In this method, the channel gain considered which is directly affected by physical installation dimensions of the room and the locations of transmitters and receivers. Binary data random generated is used for training both NN and linear regression, while the target data was the original transmitted binary data, also another data set with same specification is used for testing. The proposed NN and linear regression method feed with received signals that transmitted through the MIMO channel. Simulation results of both NN and linear regression method compared and it's clear that the BER was in range of 10^{-5} for the NN which is better than the BER for linear regression method which was in range of 10^{-2}. The main advantage of using NN for VLC channel estimation is the reduction of SNR while keeping low BER.

5.2 FUTURE WORK

As a future works the proposed channel may be compared with known practical VLC channel to satisfy the NN channel estimator accuracy.

REFERENCES

[1] M. A. Khalighi and M. Uysal, “Survey on free space optical communication: A communication theory perspective,” *IEEE Commun. Surv. tutorials*, vol. 16, no. 4, pp. 2231–2258, 2014.

[2] I. D. Association, “Serial Infrared Link Access Protocol (IrLAP),” *IrDA Publ. http//www. irda. org*, 1996.

[3] M. Nakagawa, “Visible light communications,” in *Conference on Lasers and Electro-Optics*, 2007, p. CTuI5.

[4] H. Haas, “High-speed wireless networking using visible light,” *SPIE Newsroom*, vol. 1, no. 1, 2013.

[5] Y. Tanaka, S. Haruyama, and M. Nakagawa, “Wireless optical transmissions with white colored LED for wireless home links,” in *11th IEEE International Symposium on Personal Indoor and Mobile Radio Communications. PIMRC 2000. Proceedings (Cat. No. 00TH8525)*, 2000, vol. 2, pp. 1325–1329.

[6] C.-L. Liao *et al.*, “Light-emitting diodes for visible light communication,” in *2015 International Wireless Communications and Mobile Computing Conference (IWCMC)*, 2015, pp. 665–667.

[7] A. Burton, H. Le Minh, Z. Ghassemlooy, E. Bentley, and C. Botella, “Experimental Demonstration of 50-Mb/s Visible Light Communications Using 4$\,\times\, $4 MIMO,” *IEEE Photonics Technol. Lett.*, vol. 26, no. 9, pp. 945–948, 2014.

[8] J. Armstrong, “OFDM for optical communications,” *J. Light. Technol.*, vol. 27, no. 3, pp. 189–204, 2009.

[9] Z. Ghassemlooy, L. N. Alves, S. Zvanovec, and M.-A. Khalighi, *Visible light communications: theory and applications*. CRC press, 2017.

[10] P. H. Pathak, X. Feng, P. Hu, and P. Mohapatra, “Visible light communication, networking, and sensing: A survey, potential and challenges,” *IEEE Commun. Surv. tutorials*, vol. 17, no. 4, pp. 2047–2077, 2015.

[11] H. Haas, “LiFi is a paradigm-shifting 5G technology,” *Rev. Phys.*, vol. 3, pp. 26–31, 2018.

[12] J. R. Barry, *Wireless infrared communications*, vol. 280. Springer Science & Business Media, 2012.

[13] Z. Tian, K. Wright, and X. Zhou, "The darklight rises: Visible light communication in the dark," in *Proceedings of the 22nd Annual International Conference on Mobile Computing and Networking*, 2016, pp. 2–15.

[14] S. Dimitrov and H. Haas, *Principles of LED light communications: towards networked Li-Fi*. Cambridge University Press, 2015.

[15] M. Biagi, T. Borogovac, and T. D. C. Little, "Adaptive receiver for indoor visible light communications," *J. Light. Technol.*, vol. 31, no. 23, pp. 3676–3686, 2013.

[16] J. Song, W. Ding, F. Yang, H. Yang, B. Yu, and H. Zhang, "An indoor broadband broadcasting system based on PLC and VLC," *IEEE Trans. Broadcast.*, vol. 61, no. 2, pp. 299–308, 2015.

[17] O. Ergul, E. Dinc, and O. B. Akan, "Communicate to illuminate: State-of-the-art and research challenges for visible light communications," *Phys. Commun.*, vol. 17, pp. 72–85, 2015.

[18] A. Sevincer, A. Bhattarai, M. Bilgi, M. Yuksel, and N. Pala, "LIGHTNETs: Smart LIGHTing and mobile optical wireless NETworks—A survey," *IEEE Commun. Surv. Tutorials*, vol. 15, no. 4, pp. 1620–1641, 2013.

[19] J. Luo, L. Fan, and H. Li, "Indoor positioning systems based on visible light communication: State of the art," *IEEE Commun. Surv. Tutorials*, vol. 19, no. 4, pp. 2871–2893, 2017.

[20] T. Cogalan, S. Videv, and H. Haas, "Inflight connectivity: Deploying different communication networks inside an aircraft," in *2018 IEEE 87th Vehicular Technology Conference (VTC Spring)*, 2018, pp. 1–6.

[21] B. Janjua *et al.*, "Going beyond 4 Gbps data rate by employing RGB laser diodes for visible light communication," *Opt. Express*, vol. 23, no. 14, pp. 18746–18753, 2015.

[22] Z. Ghassemlooy, W. Popoola, and S. Rajbhandari, *Optical wireless communications: system and channel modelling with Matlab®*. CRC press, 2019.

[23] D. Karunatilaka, F. Zafar, V. Kalavally, and R. Parthiban, “LED based indoor visible light communications: State of the art,” *IEEE Commun. Surv. Tutorials*, vol. 17, no. 3, pp. 1649–1678, 2015.

[24] A. Al-Kinani, C.-X. Wang, L. Zhou, and W. Zhang, “Optical wireless communication channel measurements and models,” *IEEE Commun. Surv. Tutorials*, vol. 20, no. 3, pp. 1939–1962, 2018.

[25] H. Elgala, R. Mesleh, and H. Haas, “Practical considerations for indoor wireless optical system implementation using OFDM,” in *2009 10th International Conference on Telecommunications*, 2009, pp. 25–29.

[26] J. B. Carruthers and J. M. Kahn, “Modeling of nondirected wireless infrared channels,” *IEEE Trans. Commun.*, vol. 45, no. 10, pp. 1260–1268, 1997.

[27] F. J. Lopez-Hernandez, R. Perez-Jimenez, and A. Santamaria, “Ray-tracing algorithms for fast calculation of the channel impulse response on diffuse IR wireless indoor channels,” *Opt. Eng.*, vol. 39, no. 10, pp. 2775–2781, 2000.

[28] M. Pätzold, *Mobile radio channels*. John Wiley & Sons, 2011.

[29] M. D. A. Mohamed and S. Hranilovic, “Optical impulse modulation for indoor diffuse wireless communications,” *IEEE Trans. Commun.*, vol. 57, no. 2, pp. 499–508, 2009.

[30] H. Li, X. Chen, B. Huang, D. Tang, and H. Chen, “High bandwidth visible light communications based on a post-equalization circuit,” *IEEE photonics Technol. Lett.*, vol. 26, no. 2, pp. 119–122, 2013.

[31] T. Fath and H. Haas, “Performance comparison of MIMO techniques for optical wireless communications in indoor environments,” *IEEE Trans. Commun.*, vol. 61, no. 2, pp. 733–742, 2012.

[32] S. H. Lee, K.-I. Ahn, and J. K. Kwon, “Multilevel transmission in dimmable visible light communication systems,” *J. Light. Technol.*, vol. 31, no. 20, pp. 3267–3276, 2013.

[33] S. He, G. Ren, Z. Zhong, and Y. Zhao, “M-ary variable period modulation for indoor visible light communication system,” *IEEE Commun. Lett.*, vol. 17, no. 7, pp. 1325–1328, 2013.

[34] B. Bai, Z. Xu, and Y. Fan, “Joint LED dimming and high capacity visible light communication by overlapping PPM,” in *The 19th Annual Wireless and Optical Communications Conference (WOCC 2010)*, 2010, pp. 1–5.

[35] A. E. Morra, H. S. Khallaf, H. M. H. Shalaby, and Z. Kawasaki, “Performance analysis of both shot-and thermal-noise limited multipulse PPM receivers in gamma–gamma atmospheric channels,” *J. Light. Technol.*, vol. 31, no. 19, pp. 3142–3150, 2013.

[36] O. González, R. Perez-Jimenez, S. Rodriguez, J. Rabadán, and A. Ayala, “OFDM over indoor wireless optical channel,” *IEE Proceedings-Optoelectronics*, vol. 152, no. 4, pp. 199–204, 2005.

[37] J. Mietzner, R. Schober, L. Lampe, W. H. Gerstacker, and P. A. Hoeher, “Multiple-antenna techniques for wireless communications-a comprehensive literature survey,” *IEEE Commun. Surv. tutorials*, vol. 11, no. 2, pp. 87–105, 2009.

[38] T. Fath and H. Haas, “Optical spatial modulation using colour LEDs,” in *2013 IEEE International Conference on Communications (ICC)*, 2013, pp. 3938–3942.

[39] E. Bayaki, R. Schober, and R. K. Mallik, “Performance analysis of MIMO free-space optical systems in gamma-gamma fading,” *IEEE Trans. Commun.*, vol. 57, no. 11, pp. 3415–3424, 2009.

[40] M. Brandt-Pearce and M. Noshad, “Optical transmission,” in *Academic Press Library in Mobile and Wireless Communications*, Elsevier, 2016, pp. 661–687.

[41] X. Li, R. Zhang, and L. Hanzo, “Optimization of visible-light optical wireless systems: Network-centric versus user-centric designs,” *IEEE Commun. Surv. Tutorials*, vol. 20, no. 3, pp. 1878–1904, 2018.

[42] T. Komine and M. Nakagawa, “Fundamental analysis for visible-light communication system using LED lights,” *IEEE Trans. Consum. Electron.*, vol. 50, no. 1, pp. 100–107, 2004.

[43] F. R. Gfeller and U. Bapst, “Wireless in-house data communication via diffuse infrared radiation,” *Proc. IEEE*, vol. 67, no. 11, pp. 1474–1486, 1979.

[44] K. Lee and H. Park, “Channel model and modulation schemes for visible light communications,” in *2011 IEEE 54th International Midwest Symposium on Circuits and Systems (MWSCAS)*, 2011, pp. 1–4.

[45] G. Mangqing, X. Gang, G. Jinchun, and L. Yuan’an, “Enhanced EVD based channel estimation and pilot decontamination for Massive MIMO networks,” *J. China Univ. Posts Telecommun.*, vol. 22, no. 6, pp. 72–77, 2015.

[46] S. Coleri, M. Ergen, A. Puri, and A. Bahai, “Channel estimation techniques based on pilot arrangement in OFDM systems,” *IEEE Trans. Broadcast.*, vol. 48, no. 3, pp. 223–229, 2002.

[47] Y. LeCun, Y. Bengio, and G. Hinton, “Deep learning,” *Nature*, vol. 521, no. 7553, pp. 436–444, 2015.

[48] P. Langley, *Elements of machine learning*. Morgan Kaufmann, 1996.

[49] E. Balevi and J. G. Andrews, “Deep learning-based channel estimation for high-dimensional signals,” *arXiv Prepr. arXiv1904.09346*, 2019.

[50] B. Le Saux and M. Hélard, “Iterative Channel Estimation based on Linear Regression for a MIMO-OFDM system,” in *2006 IEEE International Conference on Wireless and Mobile Computing, Networking and Communications*, 2006, pp. 356–361.

[51] P. Arena, C. Berg, L. Patané, R. Strauss, and P. S. Termini, “An insect brain computational model inspired by Drosophila melanogaster: architecture description,” in *The 2010 International Joint Conference on Neural Networks (IJCNN)*, 2010, pp. 1–7.

[52] E. Volná, “Neuronové sítě 1,” *Ostrava Ostrav. univerzita v Ostravě. Vydání druhé*, 2008.

[53] B. Yegnanarayana, *Artificial neural networks*. PHI Learning Pvt. Ltd., 2009.

[54] A. C. Guyton and J. E. Hall, “Medical physiology,” *Gökhan N, Çavuşoğlu H*, vol. 3, 2006.

[55] S. Santurkar, D. Tsipras, A. Ilyas, and A. Madry, “How does batch normalization help optimization?,” in *Advances in Neural Information Processing Systems*,

2018, pp. 2483–2493.

[56] N. Srivastava, G. Hinton, A. Krizhevsky, I. Sutskever, and R. Salakhutdinov, "Dropout: a simple way to prevent neural networks from overfitting," *J. Mach. Learn. Res.*, vol. 15, no. 1, pp. 1929–1958, 2014.

[57] A. Krizhevsky, I. Sutskever, and G. E. Hinton, "Imagenet classification with deep convolutional neural networks," in *Advances in neural information processing systems*, 2012, pp. 1097–1105.

[58] X. Yin, J. A. N. Goudriaan, E. A. Lantinga, J. A. N. Vos, and H. J. Spiertz, "A flexible sigmoid function of determinate growth," *Ann. Bot.*, vol. 91, no. 3, pp. 361–371, 2003.

[59] A. Karpathy, "Cs231n convolutional neural networks for visual recognition," *Neural networks*, vol. 1, no. 1, 2016.

[60] Y. LeCun *et al.*, "Handwritten digit recognition with a back-propagation network," in *Advances in neural information processing systems*, 1990, pp. 396–404.

[61] Y. LeCun, L. Bottou, Y. Bengio, and P. Haffner, "Gradient-based learning applied to document recognition," *Proc. IEEE*, vol. 86, no. 11, pp. 2278–2324, 1998.

[62] J. Ryu, M.-H. Yang, and J. Lim, "Dft-based transformation invariant pooling layer for visual classification," in *Proceedings of the European Conference on Computer Vision (ECCV)*, 2018, pp. 84–99.

[63] G. A. Rao, K. Syamala, P. V. V Kishore, and A. Sastry, "Deep convolutional neural networks for sign language recognition," in *2018 Conference on Signal Processing And Communication Engineering Systems (SPACES)*, 2018, pp. 194–197.

[64] A. Ng *et al.*, "Unsupervised feature learning and deep learning." Technical report, Stanford University, 2013.